Available online at **www.joac.info**

ISSN: 2278-1862

Journal of Applicable Chemistry

2019, 8 (4): 1665-1674

(International Peer Reviewed Journal)

Microwave oven Aided Synthesis and Characterization of Barium oxide Nanoparticles

I. Mallikarjuna[1], M. K Triveni[2] and T. Shivalingaswamy[3]*

1. Department of Chemistry, Maharani Science College for Women, Mysore, **INDIA**
2. Department of Chemistry, Maharaja I.T Mysore-571438, **INDIA**
3. P.G. Department of Physics, Government College (Autonomous), Mandya-571401, **INDIA**

Email: tssphy@gmail.com

Accepted on 15th June, 2019

ABSTRACT

Nano meter sized metal oxide particles draw much attention because of their unusual physical and chemical properties. They have wide range of applications in the fields of electronics, fuel cells, batteries, agriculture etc., This article focuses on the microwave oven aided synthesis and characterization of Barium oxide (BaO) nanoparticles. Synthesis has been carried out using reduction of research grade barium nitrate powder using natural gum (eucalyptus) as a fuel by solution combustion method. BaO nanoparticles were characterized by XRD for their crystallinity, shape and orientation, FTIR for their bond stretching, UV-Visible for measurement of energy band gap, EDS for their purity and SEM for their morphology. Adsorption studies are done to find the use of BaO as a base material in paints.

Graphical Abstract

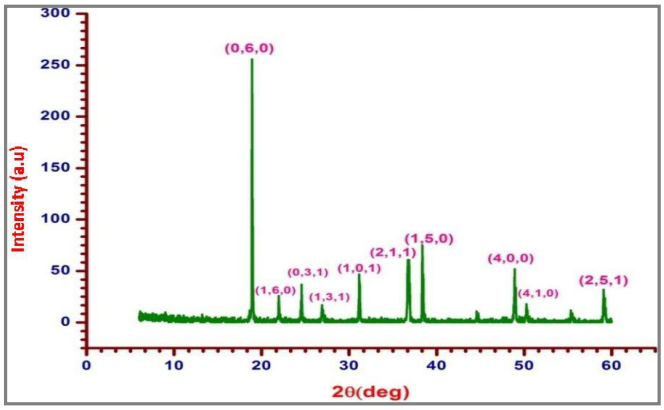

XRD plot of BaO

Keywords: Nanoparticles, Solution Combustion Method, XRD, FTIR, UV-Vis spectrometry, EDS, SEM, Dye degradation.

INTRODUCTION

Nanotechnology aims at designing and making tailored structures at the nanoscale (in the order of one to hundred nanometers) [1, 2]. The materials in the nano scale exhibit physical properties different from the bulk. For metal Nanoparticle/Nanocrystals, the energy levels become discrete, whereas, for a semiconductor the energy band gap increases significantly. This change in energy level structure is due to electron confinement effect due to which, optical, electronic and thermal properties of nanomaterials will be different from that of their bulk form [3, 4]. If a bulk material is reduced to nanoscale, the surface area enormously increases. Hence, the surface area dependent properties like catalytic activity, gas adsorption and chemical reactivity of nanostructures will deviate from their bulk form [5].

MATERIALS AND METHODS

Synthesis of nanoparticles by Solution Combustion Method: Solution Combustion Method (SCM) is a unique technique used for the synthesis of nanoparticles [6]. It is an exothermic redox reaction between a fuel and an oxidizer. The temperature provided by microwave oven and the exothermic reaction will trigger the reaction. SCM is a self-propagating high temperature process [7].

Natural Gum and Gum Extract: Natural gums are formed due to scission, injury or fungal infection. They are hydro colloidal polysaccharides, capable of causing a large increase in a solution's viscosity, even at small concentrations. In the food industry they are used as thickening, gelling, emulsifying agents, and also as stabilizers. Gum naturally oozed out of trees is collected, visible dust, other extraneous materials are removed. It is then dried for three days under sunlight. Gum is crushed to get fine powder. Required amount of sample is weighed and mixed with distilled water and thoroughly stirred for two hours to get appropriate concentration gum solutions.

Nanocrystals: Crystalline nanoparticles are referred to as nanocrystals. Nanocrystals constitute a major class of nanomaterials. Nanocrystals are zero-dimensional nanostructures possessing nano-metric dimensions in all the three space dimensions. In nanocrystals electrons are completely confined. The effect of confinement on the resulting energy states can be calculated by quantum mechanical principles, such as the "particle in the box" problem. An electron is considered to exist inside an infinitely deep potential well (region of negative energies), from which it cannot escape as is confined by the dimensions of the nanostructure. The energy of such confined electrons is given by,

$$E_n = \frac{(n_x^2 + n_y^2 + n_z^2)h^2}{8mL^2}$$

where h is Planck's constant, m is the mass of the electron, L is the width (confinement) of the infinitely deep potential well, and n_x, n_y, n_z are the principal quantum numbers in three dimensions *x*, *y* and *z* Smaller the dimensions of the nanostructure (smaller L), wider is the separation between the energy levels leading to a spectrum of discreet energies [8].

Barium oxide as nanocrystals: A. Zeenath Bazeera and M. Irfana Amrin have studied the preparation and characterization of BaO nanoparticles [9]. Preparation was carried out by thermo-chemical method using anhydrous $BaCl_2$ powder and ammonia with distilled water as a precipitant agent. The synthesized nanoparticles were characterized by XRD, FTIR spectroscopy. The XRD pattern showed that the synthesized BaO nanocrystals were of tetragonal structure with average crystalline size of 29 nm. The FTIR study confirmed that the functional groups appeared at 1610 cm^{-1} is due to Ba-O stretching mode. G. Suresh *et.al*., have synthesized, BaO nanorods by chemical bath deposition technique. They have studied the role of additives on size and shape of nanocrystalline rods [10]. T.R Machado, Livio Ferrazza and David Juanes have studied synthesis and characterization

of nano-structured BaO solutions application in preservation of wall paintings. The results indicate that the nanostructurated BaO products may have a protection on wall paint layers. The superficial application of the product forms a thin layer, compatible with the chemical nature of the wall painting and produced a consolidating action, on the surface [**11**].

Materials used: Eucalyptus gum, distilled water, Barium nitrate.

Eucalyptus gum: A survey of Eucalyptus trees was made to identify adult trees that are suitable for the collection of gum. A small wound was made on its stem and was masked by polythene material to prevent mixing of dust and other extraneous materials. Tree oozed out gum in 3-4 days. After a week, gum was collected and dried for four days under sunlight. Gum was then crushed to get fine powder. Known amount of sample was weighed and mixed with distilled water (50 mL, 100 mL, 150 mL, etc.) and thoroughly stirred to get gum solutions.

Microwave Oven Assisted Synthesis of Barium oxide nanocrystals: BaO nanocrystals were successfully synthesized by microwave oven assisted solution combustion method for which we collected Eucalyptus gum and prepared gum extract of known concentrations. $Ba(NO_3)_2$ was weighed by means of electronic balance and mixed thoroughly with appropriate gum extracts of different concentrations. The mixture was then placed in a microwave oven and heated for five minutes at a temperature of 400°C. The chemical reaction started in a minute after switching on the oven. Lot of nitrous gas is released and solution gets crystallized with cracking sound. The sample was then taken out and crushed gently and subjected for calcination process to remove volatile impurities by means of a muffle furnace operated at 700°C for three hours. The reaction can be summarized as follows

$$Ba(NO_3)_2 + H_2O \rightarrow BaO + 2HNO_3$$

The nanocrystals obtained by physical appearance are found to be as shown in the image below

Figure 1. Calcination of BaO

Figure 2. BaO nanoparticles

RESULTS AND DISCUSSION

Powder X-Ray Diffraction: XRD technique is the most common and efficient method to determine structure and crystallinity [**12**]. Crystalline phases can be identified by just comparing the inter planar distance 'd' values obtained from XRD data with the fundamental data in Joint Committee on Powder Diffraction Standards (JCPDS). The Debye-Scherrer equation is used to estimate the size of submicro crystallites. The Scherrer equation can be written as:

$$d = \frac{K\lambda}{\beta cos\theta}$$

Where, d is the mean size of the ordered domains which is equal to the grain size. k is a dimensionless shape factor, called crystalline shape factor which is best approximated to 0.89. λ is the wavelength of X-ray. β is the full width at half maximum (FWHM) in radians.

XRD measurements were carried out at room temperature using RIGAKU smart lab X-ray diffractometer at Institute of Excellence (IOE), University of Mysore with monochromatic beam of Cu − Kα radiation 1.5406 Å.

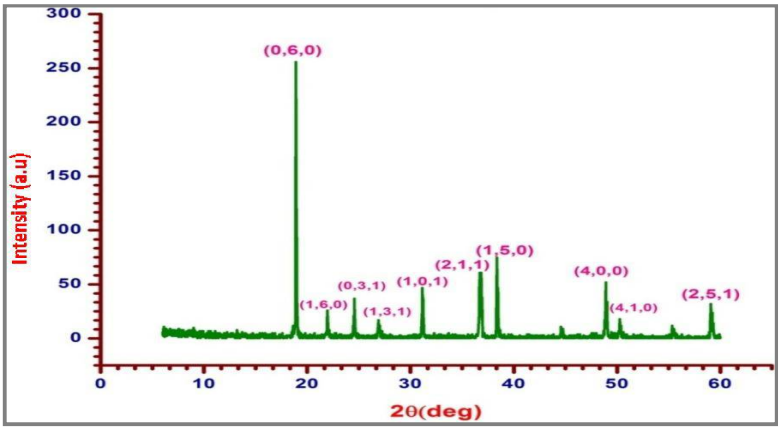

Figure 3. XRD plot of BaO.

An accelerating tube voltage of 40 KV and a tube current of 15 mA with a scanning speed 0.01 to 100° m^{-1} and scanning range 0 to 140° (2θ). Ultra detector with accuracy +0.02° were used. The XRD patterns were recorded; the values of 2θ, d- spacing, relative intensity and FWHM were obtained from the XRD pattern. Identification of phases was carried out by comparing the diffraction pattern obtained from XRD with standard JCPDS database (File no.89-8425). Further, on comparison with JCPDS database file we found that BaO belong to tetragonal crystal system [**13, 14**]. W-H Plot is used to determine crystal size broadening. This method is attributed to G. K. Williamson and his student, W. H. Hall. It is based on the principle that the approximate formula for size broadening and strain broadening vary quite differently with respect to Bragg angle (θ):

$$\beta_L = \frac{k\lambda}{Lcos\theta} \text{ and} \beta_e = C_e \tan\theta$$

If both contributions are present then their combined effect should be determined by convolution. The simplification of W-H method is to assume the convolution as a simple sum. Using the former of these then we get:

$$\beta = \beta_e + \beta_L = C_e \tan\theta + \frac{k\lambda}{Lcos\theta}$$

If we multiply this equation by cosθ we get:

$$\beta \cos\theta = C_e \sin\theta + \frac{k\lambda}{L}$$

Comparing this with the standard equation for a straight line y = mx + c, we see that by plotting β cosθ versus sinθ we obtain the strain line with the slope Cϵ and the intercept kλ /L cos θ that determines size of the crystal. Such a plot is known as a W-H plot.

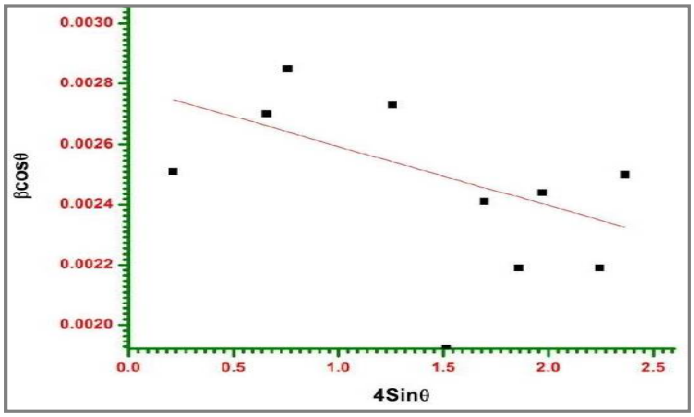

Figure 4. W-H Plot for Barium Oxide.

Determination of crystal sizes are made using Scherer's method and W-H plot for BaO nanocrystals, the average crystal sizes are found to be 50:01*nm* and 49:33*nm* respectively.

Table 1. XRD data analysis for crystal size determination

2θ	θ	$Sin\ \theta$	β	BCosθ	$d = \frac{K\lambda}{\beta cos\theta}\ nm$	W-H Plot $d = \frac{k\lambda}{C}$
18.9019	9.450	0.164	0.156	0.1538	51.046	
21.9511	10.975	0.190	0.166	0.1629	48.194	
24.5799	12.289	0.212	0.195	0.1905	41.216	
26.8642	13.432	0.232	0.174	0.1692	46.402	
31.1485	15.574	0.268	0.187	0.1801	43.59	49.33
36.6957	18.347	0.314	0.189	0.1794	43.77	
36.8492	18.424	0.316	0.157	0.1489	53.72	
38.3704	19.185	0.328	0.164	0.1154	50.70	
48.9235	24.461	0.414	0.149	0.1356	57.90	
50.2800	29.535	0.492	0.142	0.1235	63.53	
					d_{avg}= 50.01	

The Lorentz factor is a trigonometric factor that relates to the distribution of planes as a function of θ. For a powder sample, with randomly oriented crystals, the integrated intensity (area under the curve) of a reflection at a given Bragg angle depends on the number of particles with that orientation. Even though the particles are oriented at random this number is not a constant, but it depends on the value of the Bragg angle. This dependence is called the Lorentz factor and is given by,

$$\text{Lorentz factor} = \frac{1}{4sin^2\theta cos\theta}$$

Generally, the Lorentz factor is combined with the polarization factor to form
The Lorentz-polarization factor

$$\text{Lorentz polarization factor} = \frac{1 + Cos^2\theta}{sin^2\theta cos\theta}$$

The Lorentz-polarization factor as a function of Bragg angle is useful in determination of crystal orientations in a powder sample.

Temperature factor: Atoms in the lattice are constantly vibrating about their equilibrium position. As the temperature increases, the amplitude of vibration increases. One effect of this vibration is that

the lattice spacing constantly changes so that the overall intensity of a line decreases with increasing temperature, at the same time background scattering increases. For a given temperature the effect is pronounced at higher Bragg angles since the d-spacing is smaller. The temperature effect is usually determined experimentally and written as

$$T_f = \exp\left[B\left(\frac{sin\theta}{\lambda}\right)^2 \right]$$

Where the best approximation of $B = 0{:}5$

The Lorentz-polarization factor as a function of Bragg angle is plotted for BaO nanocrystals, the plots are as shown below. From the plot, it is clear that there are random orientations of the crystals and more crystal orientation is found at an angle around 60◦. Further from temperature factor plot it is clear that the logarithmic value of temperature factor with respect to 2θ is a straight line as expected.

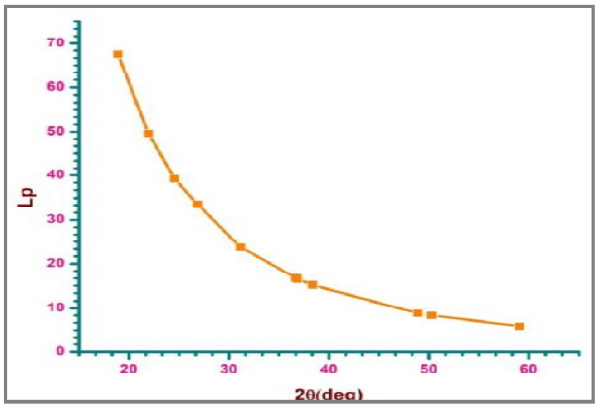

Figure 5. *Lp* Vs 2θ

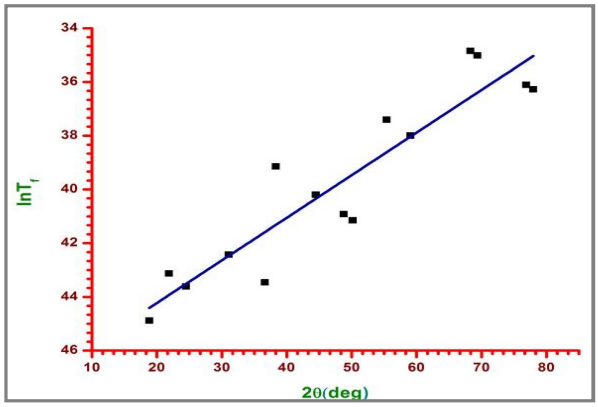

Figure 6. ln T_fVs $2\,\theta$

Fourier Transform Infrared Spectroscopy: FTIR Measurements were carried out at room temperature using FTIR- 4100 type-A model of serial number B110861016, TGS detector with standard light source of resolution 16 cm^{-1} and scanning speed-Auto (2 mm sec^{-1}) with filter-auto (3000Hz), it was found that the functional groups appeared at 1602 cm^{-1} is due to the Ba-O stretching mode.

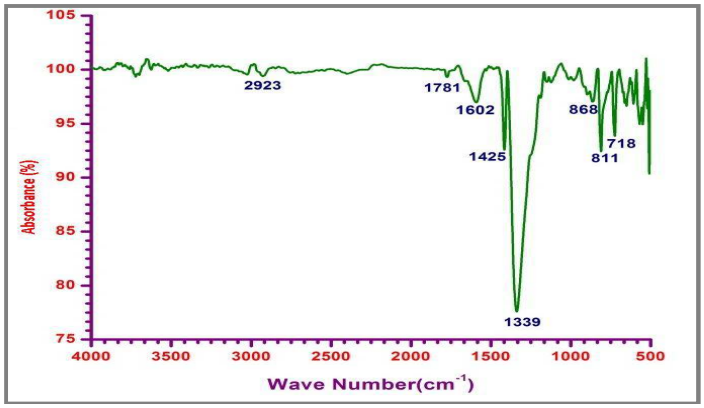

Figure 7. FTIR Spectrum.

UV-Visible Spectroscopy: The measurement of the band gap of materials is important in nanomaterials to find their suitability of application. UV-Visible spectroscopy is an important tool to

measure energy band gap of the nanocrystals [**15**]. By identifying peak wavelength of energy absorption, one can find the energy band gap in the nanocrystals using the relation,

$$E = \frac{hc}{\lambda_{max}}$$

Where, h = planck's constant, c = speed of light and λ_{max} = peak wavelength of absorption. UV-Visible spectrometry was carried out at room temperature using UV-Visible spectrometer lab tronics MODEL LT-291 with single beam of range from 200 nm to 900 nm for BaO samples prepared with different concentrations. This characterization is done using the facility available at P.G. department of Physics, Government College (Autonomous), Mandya. From the absorbance peak we have estimated the energy band gap of BaO samples and are shown in the table 2.

The energy band gap is found to increase with the increase in concentration as expected. Further, the value of energy band gap confirms that BaO nanocrystals are insulating materials.

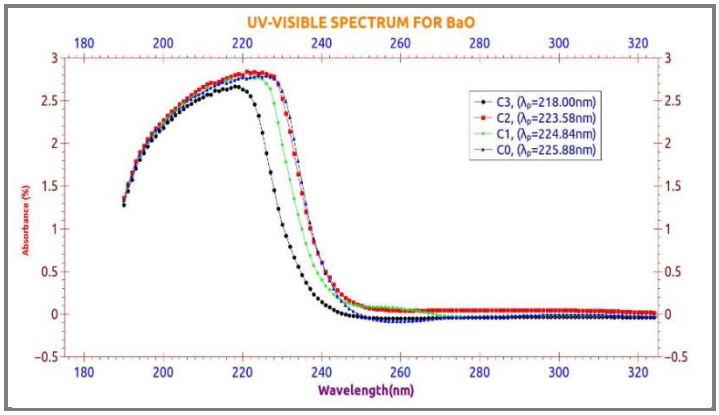

Figure 8. UV-Visible spectrum of Barium Oxide.

Table 2. Determination of Energy band gap for different gum concentration of BaO Nanocrystal

BaO concentration	λc	($Eg = 10^{19}$) (joules)	Eg (eV)
10%	225.88	8.8002	5.5001
15%	224.84	8.8409	5.5255
20%	223.58	8.8907	5.5567
25%	218.00	9.1183	5.6989

Energy Dispersive Spectroscopy: EDS or EDX study was made using energy dispersive spectrometer, Hitachi model S-3400N with magnification range 5X to 300,000X. From the elemental analysis we find that the obtained BaO nanoparticles are in pure form (Figure 9).

Scanning Electron Microscopy: A scanning electron microscope (SEM) produces morphological images of a sample by scanning the surface with a focused beam of electron. The SEM analysis was done using SEM Hitachi model S-3400N with magnification range 5X to 300,000X.

Table 3. Elemental analysis of BaO Nanocrystal after calcination

Elemental line	Weight	Error in weight	Atomic(percentage)
O K	30.12	0.74	78.72
Ba L	69.88	2.19	21.28
Total	100.00	--	100.00

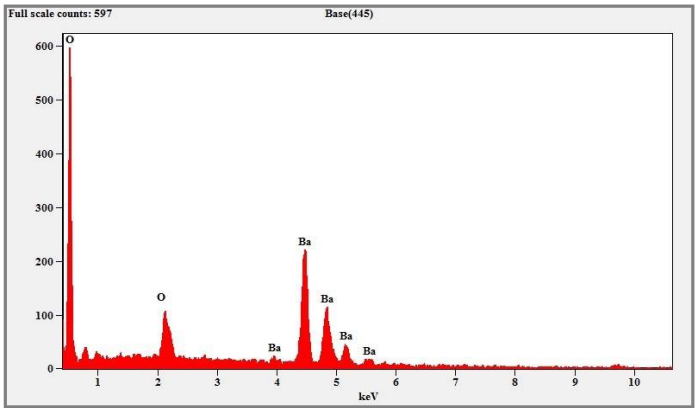

Figure 9. EDX image of BaO nanocrystals.

The morphology of the BaO was found to be as shown in the figure below. SEM images of BaO derived from gum extract of Eucalyptus showed agglomerated pattern with an average size of 40 nanometer. However, this agglomeration has been removed by dispersing these nanocrystals in water and shaking the mixture in ultrasonic desiccators followed by calcination process. After this process, we get nanocrystals which are well distinguished without any agglomeration. This may be due to fact that, some of the volatile impurities present in the sample provide weak bonds leading to agglomeration of the sample. However, the rigorous shaking of this in ultrasonic desiccators will help in breaking these week bonds. Further, heating the substance at high temperature ($600^{\circ}C$) removes volatile impurities. Thus the output is fine nanocrystals.

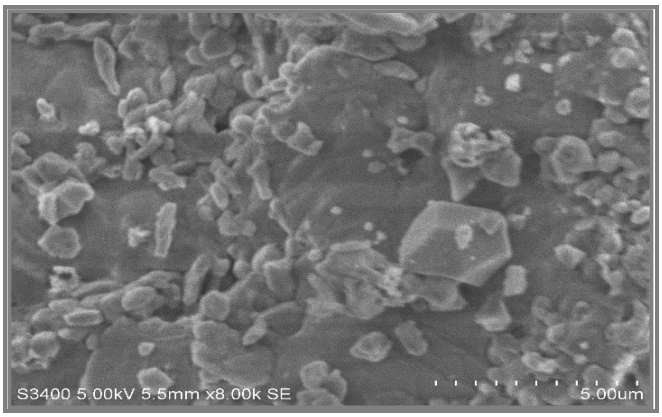

Figure 10. SEM image of BaO nanocrystals.

Dye degradation studies of BaO: The surface chemistry of any material is determined by the acidic or basic character of its surface. It is very important to know the surface charge of the material in the aqueous media. Therefore, it is necessary to find the point of zero charge or zero point charge pH(pzc) of the adsorbent material [**16**].

Determination of surface charge: Point of zero charge or the isoelectric point is the pH (pzc) of the solution at which the total charge on the surface of nanoparticles becomes zero(neutral). The pzc of BaO was measured by pH drift method. In this method, 50 mL of 0:01 M of solution was taken in six separate beakers. The pH of the solution in each beaker was adjusted between 2 and 12 by adding HCl or NaOH after which 150 mg of adsorbent ie., Barium oxide was added to the solutions. Each of them was kept for shaking at 200 rpm for 48 h or until stable pH was obtained. The final pH was measured and a graph of initial pH vs final pH was plotted. The point at which this curve crosses the initial pH = final pH straight line is the point of zero charge. The pzc obtained for BaO is 6.4.

The surface charge of the BaO is 6.4. This means that the surface of Bariumoxide nanoparticles is basic in nature below the pH (pzc) and acidic above. The pH of aqueous indigo carmine is below the pH (pzc) of the BaO material which favors the adsorption of anionic indigo carmine and thus is suitable for photo catalysis. A blank experiment was conducted to ensure that there no degradation of aqueous indigo carmine under Visible light irradiation.

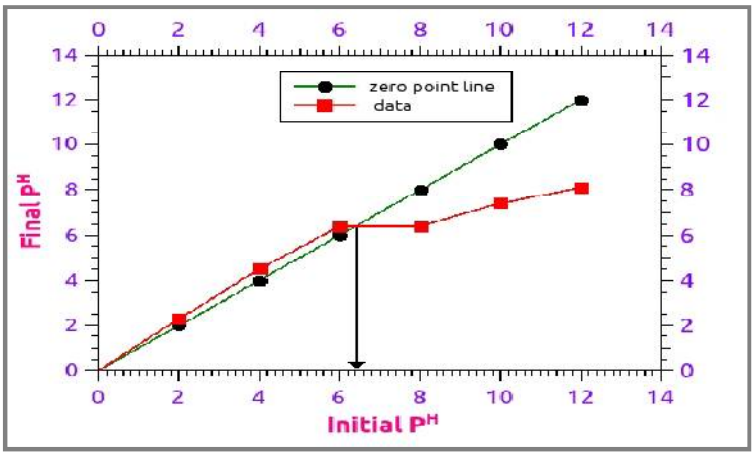

Figure 11. Zero point charge graph.

Photo catalytic activity: Photo catalytic efficiency of BaO nanoparticles was evaluated by measuring the degradation of aqueous indigo carmine under Visible lamp(125W Hg lamp as source) irradiation. 0.02 g of catalyst was added to the 25mL of the 1 x 10^{-4} M aqueous solution of indigo carmine at pH 2. The mixture was stirred in dark for one hour to reach adsorption and desorption equilibrium before subjecting to visible lamp 3h. The dye concentration was monitored spectrophotometrically at 615nm, where the absorbance is maximum for indigo carmine. The degradation efficiency of the dye was treated in the form of percentage of dye degradation and it was found to be 50.88%.

Table 4. Decrease of absorbance of indigo carmine with increase of time and showing Photo catalytic activity of BaO

Time in minutes	Absorbance	Degradation (%)
0	1.461	
10	1.135	
20	1.320	
30	1.223	
40	1.220	
50	1.043	
60	0.971	50.88
70	0.864	
80	0.755	
90	0.744	
100	0.744	
110	0.734	
120	0.730	
130	0.728	
140	0.726	
150	0.722	

APPLICATION

The measured character of BaO nanoparticles indicate that it could serve as a better photo catalytic substance for degradation of certain dyes.

CONCLUSION

In this work we have successfully synthesized BaO nanoparticles by using solution combustion method with the aid of microwave oven. They are characterized by different characterization tools such as XRD, EDS, SEM, UV-Vis FTIR etc. Various physical properties, such as, size, orientation, bond stretching, purity, energy band gap, morphology etc. are determined.

As an application, we have also done dye degradation test to check its suitability in paint as an adhesive. Further it would be better if some electrical, magnetic and thermal characterizations are done to widen its role in applied sciences. This work would be taken up in the due course.

ACKNOWLEDGEMENTS

The authors thank B.C. Karigowda, M. Ramegowda, M.R. Nandan, A. Raghu, K.M. Eshwarappa and B.S. Palakshamurthy for their support. Further our special thanks to our M.Sc students A. Akhila, B. Hema, R. Kavya and J.M. Pallavifor their help in the research work

REFERENCES

[1]. J. M. Taylor, New Dimensions for Manufacturing: Report for the UK Advisory Group for Nanotechnology applications,London,http://www.dti.gov.uk/innovation/nanotechnologyreport.pdf. **2002**.
[2]. M. L. Steigerwald, L. E. Brus, *Acc. Chem. Res.*, **1990**, 23, 183.
[3]. C. Burda, X. Chen, R. Narayanan, M. A. El-Sayed, *Chem. Rev.*, **2005**, 105,1025.
[4]. P.V. Kamat, *Chem. Rev.*, **1993**, 93, 267.
[5]. M. R. Hoffmann, S. T. Martin, W. Choi, D.W. Bahnemann, *Chem.Rev.*, 1995, 95, 69.
[6]. Singanahally T. Aruna, Alexander S.Mukasyan, *Current Opinion in Solid State and Materials Science*, **2008**, 12(3), 44.
[7]. Jiachun Deng, Litao Kang, Gailing Bai, Ying Li, Xuguang Liu, Yongzhen Yang, Feng Gao, Wei Liang, *ElectrochimicaActa*, **2014**, 132, 127
[8]. T. Pradeep *et.al*., *A Text book of Nanoscience and Nanotechnology*, TataMcGraw Hill Education Private Limited, New Delhi, Part four, **2012**.
[9]. A. Zeenath Bazeera, M. Irfana Amrin, *IOSR-Journal of Applied Physics*, **2017**, 76,
[10]. Gopalakrishnan Suresh, Putta Narasimhan Nirmala, *Turk. J. Phys.*, **2012**, 36, 392.
[11]. Elisa Cordoncillo, T. R. Machado, Livio Ferrazza, David Juanes, *Euro Med*, **LNCS 7616**, Springer-Verlag Berlin Heidelberg, **2012**, 801.
[12]. J. K. Flohr, *X-ray Powder Diffraction*, Francis. A. F. Science for A Changing World, **1997**, 53.
[13]. Camden R. Hubbard, *Standard X-ray Diffraction Powder Patterns Section18-Data for 58 Substances*, National Measurement Laboratory, National Bureau of Standards Washington, DC **1981**, 20234, 11.
[14]. Chauhan A, Chauhan P , *J Anal Bioanal Tech*, **2014**, 5, 212.
[15]. K.R. Nemade, S.A Waghuley, *Results in Physics*, **2013**, 3, 52.
[16]. S. Muthukrishnan, S. Bhakya, M. Sukumaran, M. Muthukumar, T. SenthilKuma, M. V. Rao, *Journal of Bioremediation and Biodegradation*, **2015**, 6, 312.